Bull. Spec. Astrophys. Obs., 2002, 53, 5–17

Photometric study of the GRB 000926 host galaxy field with the SCORPIO at the 6 m telescope

T.A. Fatkhullin

Special Astrophysical Observatory of the Russian AS, Nizhnij Arkhyz 369167, Russia

Received February 18, 2002; accepted March, 14, 2002.

Abstract. We present the results of a deep photometric study of the GRB 000926 host galaxy field with a newly designed instrument SCORPIO at the 6 m telescope of SAO RAS. The expected potentialities of using this new device in the photometric mode are demonstrated. It is shown that the limiting magnitudes ($S/N = 3$) of B=27.0, V=26.3, R_C=26.4 and I_C=25.1 are achieved. We also present the results of the BVR_CI_C photometry of the host galaxy of GRB 000926 itself. For the objects in the field the classification "star-like – extended" is performed, and for each class an attempt of classification by their colors is made. It is shown that the colors of the host galaxy correspond to those of the extended objects in the field with the same magnitudes. Moreover, the colors of the host galaxy are located in the "blue part" of the color distribution of the objects, which is explained by vigorous star formation in the host galaxy.

Key words: gamma rays: bursts — galaxies: photometry

1. Introduction

Recently, accumulation of the statistics for the gamma-ray burst (GRB) afterglow and its host galaxies has shown that most probable progenitors of GRB are massive stars. This, in turn, stimulated interests in GRBs, the events which are closely related to star formation history (SFH) in the Universe (see, e.g., Blain & Natarajan, 2000; Ramirez-Ruiz et al., 2000, and references therein). Today there are many methods, which differ in the working spectral range, for estimation of SFH effects. Each of the methods has its own advantages and drawbacks. For example, studies in optics are most sensitive, but strongly affected by internal extinction in galaxies; radio methods, in turn, are free from this selection effect, but are still less sensitive than optical, and thus give only part of all information (see review of Adelberger & Steidel (2000)). Studies of GRB host galaxies are an additional independent method of SFH determination. Following the report of Berger (2001), we repeat here the main advantages of this method:

1. GRBs are bright events and, consequently, it is possible to detect them to high redshifts. Thanks to the wide spectral range of the afterglow (from X-ray to decimeter radio), it is possible to precisely localize not only a host galaxy, but to accurately measure the distance using optical spectra of the afterglow and host galaxies.

2. In fact, dust does not affect the outcoming gamma radiation, thus it is possible to create a sample of galaxies free from the influence of dust.

3. The already accumulated data are sufficient to assert that the sample of GRB host galaxies occupies a wide range of luminosities, to $M_B \sim -15^m$ (see Fig. 1 from Berger, 2001). In contrast to this, current methods of SFH estimation reach luminosities of the order of L_*, the "knee" of the local luminosity function.

As it was noted, GRB host galaxies occupy a wide range of both luminosities and apparent magnitudes (Sokolov et al., 2001). It is clear, faint objects need deep photometric studies. Thus, as an expected "by-product" of host galaxy studies may be deep fields. Clearly, these observational data contain many possibilities for different kinds of science activities, that is construction of the luminosity function in relation to redshift, search for certain kinds of objects (neutron stars, distant galaxies, transient events, etc.), number counts and so on.

In this paper we present the results of photometry of objects in the GRB 000926 host galaxy field. The structure of the paper is as follows: in the first Section we describe the method of deep photometric observations with the SCORPIO ("Spectral Camera with Optical Reducer for Photometrical and Interferometrical Observations", see at `http://www.sao.ru/~moisav/scorpio/scorpio.html`); in the second one we present the data reduction and the technique of photometry we used; in the third

© Special Astrophysical Observatory of the Russian AS, 2002

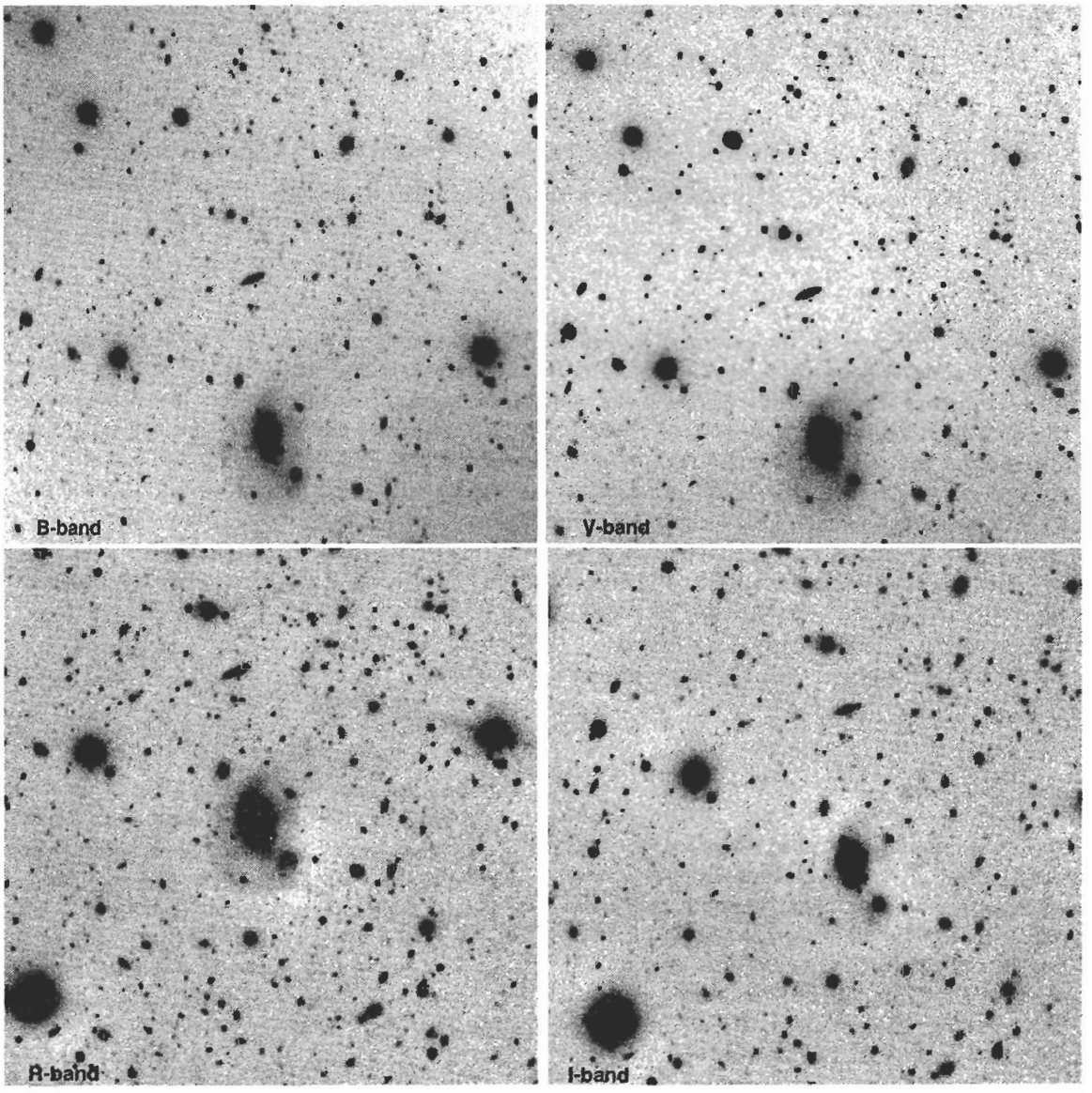

Figure 1: *The GRB 000926 host galaxy field in the B, V, R_C and I_C bands. The size of the fragments is slightly different, but about* 4.3×4.3 *arcmin.*

section we describe the results of studies for field objects and for the GRB 000926 host galaxy itself. In the last section we present conclusions.

2. Observations

Observation of the GRB 000926 host galaxy field was performed in the frame of the observational program of Sokolov V.V. "Optical identification of gamma-ray bursts", which is in progress at the 6 m telescope of SAO RAS. The data were obtained with the SCORPIO instrument and a CCD matrix detector of 1034×1034 pixels, 24×24 μm in size (corresponding to a spatial resolution of about $0.''289$/pixel) with a read-out-noise of 3 electrons and a 1.2/ADU gain. A set of filters close to the standard BVR_CI_C Johnson-Kron-Cousins photometric system (Bessel, 1990) was used. The weather conditions were good. In Table 1 the night log of the observations is presented. The standard stars from the list of Landolt (PG1633, 1992) and Stetson (`http://cadcwww.dao.nrc.ca/cadcbin/wdb/astrocat/stetson/query`) were used for photometric calibration.

It should be noted that images obtained with thin CCD detectors are not free from fringes (interference "pattern"), especially in the red part of the spectrum. To eliminate these artifacts, a dithering method was used in the course of working out technique of observations with the SCORPIO. The telescope was shifted between exposures. This makes it possible to construct a superflat image, containing the fringe pattern

Table 1: *The observational log of the GRB 000926 host galaxy field*

Date, UT	Band	Seeing FWHM	Zenithal distance	Exposure and frame numbers	Total integration time, sec
25. July, 2001	B	1.″3	34°	500 × 5	2500
25. July, 2001	V	1.″3	28°	300 × 7*	1500
24. July, 2001	R_C	1.″2	11°	180 × 7	1260
25. July, 2001	I_C	1.″3	10°	120 × 15	1800

*Two frames are with a problem of seeking. These frames were not used.

Table 2: *Results of reduction*

Band	Integration time (sec)	Sky brightness $(\frac{DN}{s \cdot pix})$	Sky brightness $(\frac{mag}{\square''})$	Atm. extinction* $(\frac{mag}{air\ mass})$
B	2500	4.19	22.69	0.34
V	1500	8.46	21.76	0.21
R_C	1260	24.76	21.16	0.15
I_C	1800	75.69	18.99	0.10

* The extinction coefficients were assumed from Neizvestny (1983).

of the CCD matrix signal, making use of median averaging, for instance. Fringes being an additive component of a CCD image, superflat is to be subtracted from the reduced frames. This procedure was applied in these observations.

3. Data reduction and photometry

Primary data reduction was performed using the `MIDAS` package. The data were bias-subtracted, flat-fielded and corrected for fringes in the R_C and I_C bands. Cosmic ray events were removed using the `MIDAS` routine `FILTER/COSMIC`. Then the frames in each band were summed. The seeing (FWHM) in the sums is 1.3, 1.3, 1.2 and 1.3 arcsec in the B, V, R_C and I_C bands, respectively. In Table 2 and Fig. 1 the results of the reduction and the fields in the B, V, R_C and I_C bands are presented.

As fields in different bands had different orientation relative to the world coordinate system, we transformed all final frames to the same coordinate system using the `WCStools` package and `USNO-A2.0` astrometrical catalog. The mean astrometrical error was about 0.5 arcsec. In Fig. 2 the intersection of all bands is presented (common field). The total area of the intersection is about 12 arcmin^2.

To transform instrumental b, v, r, i magnitudes to the standard BVR_CI_C, we make use of the following equations:

$$\begin{aligned} B - b &= 26.82(\pm 0.01) + 0.16(\pm 0.02) \cdot (b - v), \\ V - v &= 26.82(\pm 0.01) - 0.07(\pm 0.02) \cdot (b - v), \\ R_c - r &= 27.29(\pm 0.02) + 0.03(\pm 0.05) \cdot (v - r), \\ I_c - i &= 26.25(\pm 0.02) + 0.11(\pm 0.04) \cdot (r - i), \end{aligned}$$

where the tranformation coefficients were determined with the aid of the standard stars from the PG1633 field (see Sect. 2).

For searching out and photometry of objects in the field, we used the `SExtractor` routine (`Source Extractor`, Bertin and Arnouts, 1996). The `SExtractor` allows one to measure several kinds of magnitudes. For these reasons, we present here a short summary of the `SExtractor` measurement algorithm. The `SExtractor` defines the following magnitudes:

- Isophotal magnitude which is integral within the area above the given threshold.
- Corrected isophotal magnitude which is measured by the following methods. Intensity profile of an object is approximated by Gaussian and then a corresponding correction of measured magnitude is applied.
- "Automatic" (adaptive aperture) magnitude which has been defined by Kron (1980). First, a "first moment" $r_1 = \frac{\sum rI(r)}{\sum I(r)}$ is calculated. Kron showed that for star-like and galaxy profiles convolved with Gaussian, about 92% of light is enclosed within an aperture of kr_1 radius, where $k \approx 2$. In `SExtractor` an algorithm is worked out, where the aperture is presented by an ellipse with $\epsilon k r_1$ and kr_1/ϵ as major and minor axes (ϵ is the ellipticity).
- Aperture magnitude which is the magnitude measured within a circular aperture specified by the user.

The total magnitude is defined to be equal to "automatic" one provided that there is no object with a magnitude capable of increasing the total magnitude by more than 0.1^m in the corresponding aperture. On

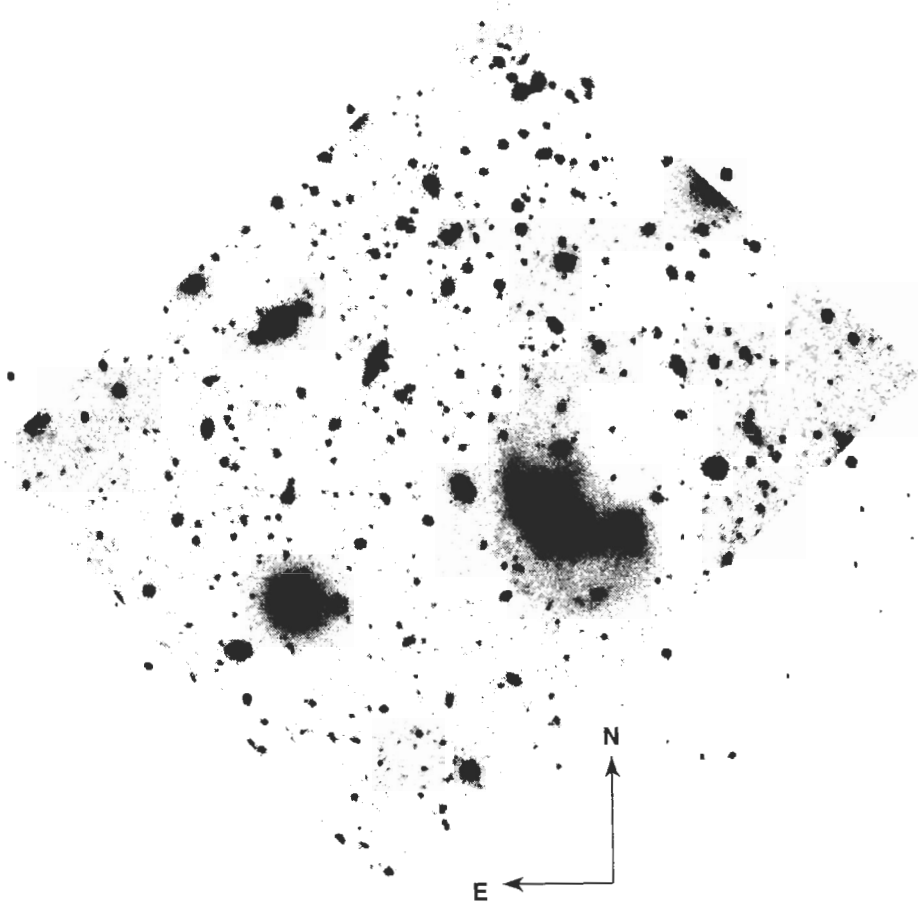

Figure 2: *The field common for all bands.*
Field corner coordinates:
North: $\alpha_{2000.0} = 17^{\rm h}04^{\rm m}06\overset{\rm s}{.}82$, $\delta_{2000.0} = +51°49'49\overset{''}{.}4$
East: $\alpha_{2000.0} = 17^{\rm h}04^{\rm m}24\overset{\rm s}{.}42$, $\delta_{2000.0} = +51°47'24\overset{''}{.}8$
South: $\alpha_{2000.0} = 17^{\rm h}04^{\rm m}10\overset{\rm s}{.}97$, $\delta_{2000.0} = +51°45'04\overset{''}{.}7$
West: $\alpha_{2000.0} = 17^{\rm h}03^{\rm m}52\overset{\rm s}{.}30$, $\delta_{2000.0} = +51°47'47\overset{''}{.}4$.

the contrary, a corrected isophotal magnitude is selected.

The detection threshold was chosen to be 1.5σ of background fluctuation (σ — RMS of background statistics). This corresponds to 27.56, 26.64, 26.62 and 25.22 magnitude per arcsec in the B, V, $R_{\rm C}$ and $I_{\rm C}$ bands, respectively ($\sim 1\%$ of the sky brightness). We triggered positive detection, when the object occupied of at least 5 pixels connected one-by-one with intensity of each of the above given thresholds. Approximation of the background is a very important procedure in searching for objects automatically. Here we examined this procedure "by eye". The approximated background was checked for the absence of structures around bright objects and sharp variation on small scales (less than $\sim$ 5–7 FWHM).

A total of 1243, 1026, 1244 and 1025 objects were found in the B, V, $R_{\rm C}$ and $I_{\rm C}$ bands, respectively. Note, these catalogs may contain spurious detections because of the effects of the backround noise. In the resulting catalog the isophotal, "total" and aperture magnitudes were measured for each object (see Bertin and Arnouts, 1996). An object with a $S/N = 3$ being assumed to be the limit of detection (internal magnitude error is ≈ 0.36), the limiting magnitudes are 27.6, 26.8, 26.8 and 25.6 in the B, V, $R_{\rm C}$ and $I_{\rm C}$ bands, respectively. But a more reliable limit was defined as the mean magnitude of objects with the given S/N ratio. Thus for $S/N = 3$ the limiting magnitudes are 27.0, 26.3, 26.4 and 25.1 in the B, V, $R_{\rm C}$ and $I_{\rm C}$ bands, respectively. In Fig. 3 we present "magnitude–error" diagrams for all detected objects with a S/N greater than 3. Objects with limiting magnitudes were examined "by eye", and we found that some of them are probably spurious detections. These objects were ruled out from the final catalog. In Fig. 4 the examples of objects with limiting magnitudes are presented.

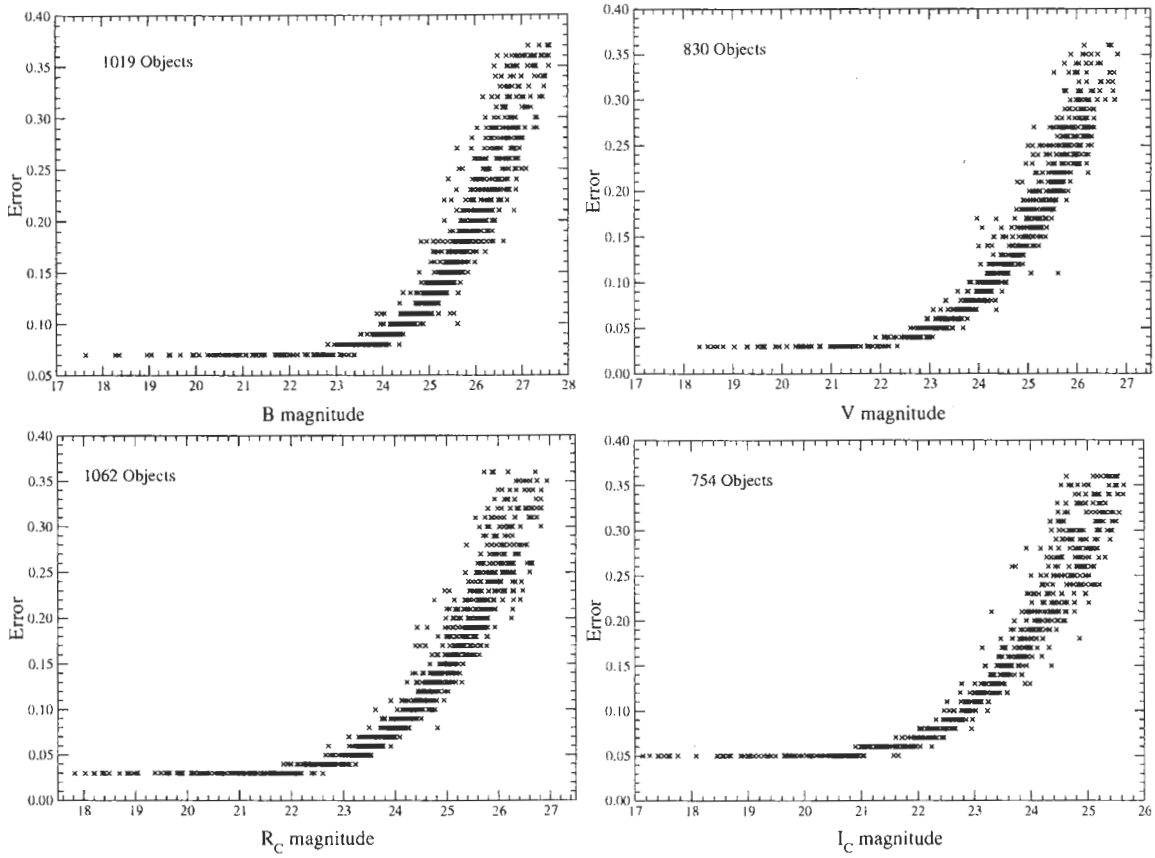

Figure 3: *The "magnitude–error" diagrams for all field objects with $S/N > 3$.*

4. Results

4.1. Number counts

Field photometry of the objects allowed us to construct the "magnitude–counts" distributions. In Fig. 5 we present the results for objects with a $S/N > 4$. Following the definition of limiting magnitude from Sect. 3, we found that for this sample the limiting magnitudes are 26.6, 25.9, 26.1 and 24.7 in the B, V, R_C and I_C bands, respectively. It should be noted that for correct interpretation of these results, in particular the slope, we need a completeness curve, but this is beyond the scope of this paper.

4.2. Object colors in the common field

Now we will deal with the objects, which have been detected simultaneously in all the bands. To match coinciding objects, we used the `IRAF` package and its tasks from `STSDAS`. The astrometrical error of our frame referring to the world coordinate system was about 0.5 arcsec, thus the confidence region we defined is one arcsec (about 3 pixels). For analysis of the data we defined a sample of objects in the common field with a $S/N > 4$. This sample consists of 192 objects. The detection in all the bands allows us to consider with assurance that an object is real, because of different orientation of the field in the different bands, which, in turn, suggests that there is not any correlation with the flat-field pattern or CCD bad pixels.

In Fig. 6 and Fig. 7 we present the two-color and "magnitude–color" diagrams for all objects of this sample. As colors are correctly measured within the same aperture in all the bands, for analysis of the colors we chose the aperture magnitude. The apperture size was defined as 12 pixels, which is 3.6 arcsec or $\approx$ 3FWHM of a star-like profile.

In Figs. 8 and 9 examples of the reddest and bluest objects in the common field are presented.

4.3. Star-like objects

To select star-like objects, we used the criterion given in `SExtractor`. We selected the objects which have the index of stellarity greater than 0.7 in all the bands (`SExtractor STAR CLASS`). There are 15 such objects. In Fig. 10 we show a two-color diagram for all star-like objects in the common field. To classify the objects, we compared the object colors with those of star spectra from the Vilnus library. Fig. 10 shows our classification of the objects. As can be seen from

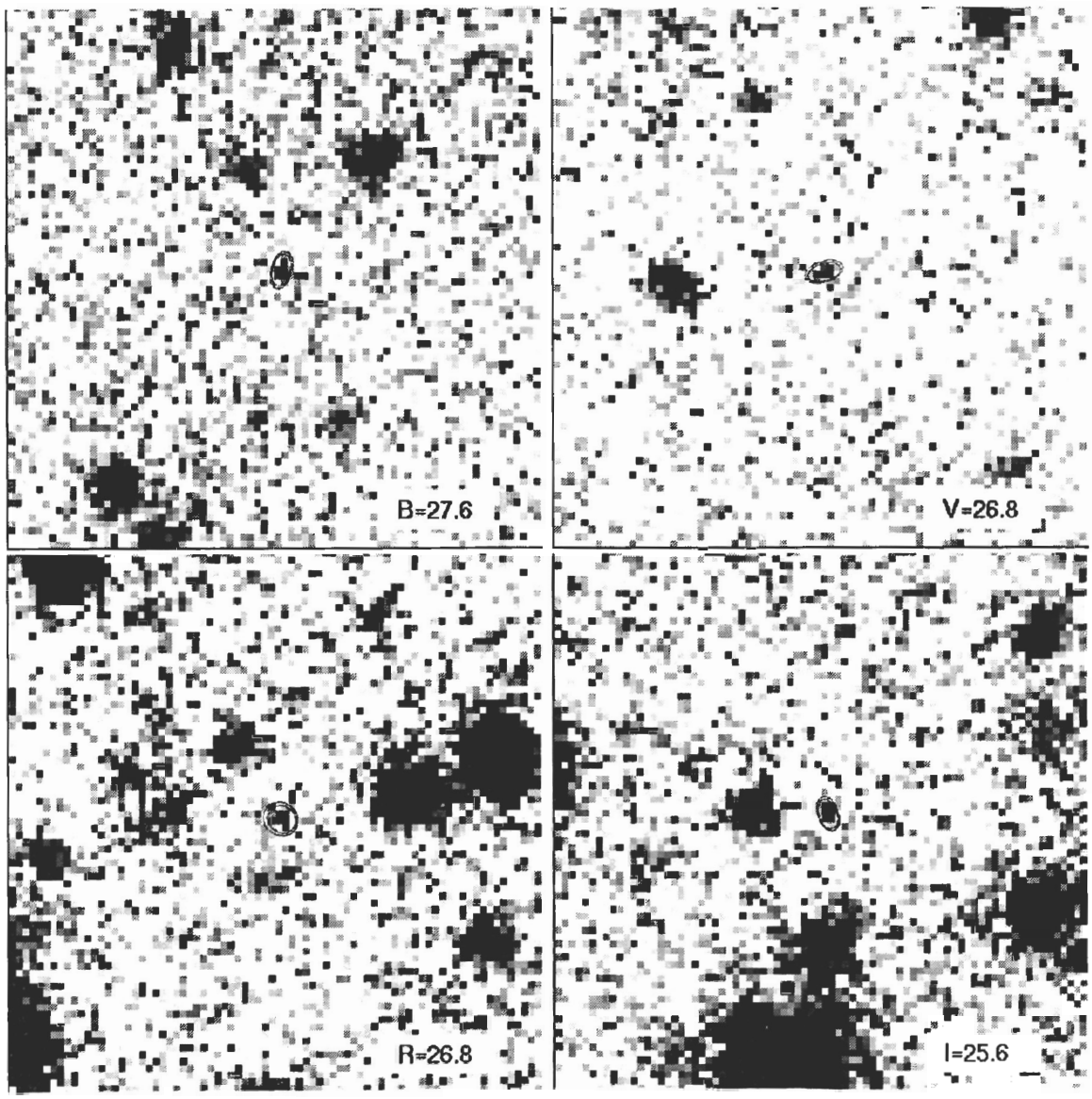

Figure 4: *Objects with limiting magnitudes. Ellipses mark apertures within measurements were performed. Inner ellipse approximately corresponds to isophotal object size, outer is total magnitude apperture.*

the figure, the colors of almost all objects are well represented by the colors of main-sequence dwarfs.

4.4. Extended objects

The colors of the extended objects (those that do not fall within the class of star-like ones on the basis of the criterion from 4.3) are compared with the colors of the galaxies of different Hubble types from Fukugita et al. (1995) at different redshifts. In Fig. 11 we show this comparison for two-color diagrams. As it can be seen from the figure, the colors of the majority of the extended objects correspond to those of galaxies with redshifts up to ~ 1. However, there are objects which need more detailed studies.

4.5. Host galaxy of GRB 000926

In Fig. 12 the 30 × 30 arcsec neighbourhood of the GRB 000926 host galaxy is shown. Using `SExtractor`, we succeeded in detecting the host galaxy in the B band only. In the V and R_C bands the algorithm, probably, did not resolve the galaxy and the nearby extended structure (see Fig. 12), in the I_C band there was no detection at all. The photometry of the host galaxy was performed by hand using the `MAGN/CIRCLE` procedure in the `MIDAS` package. Within the 2-arcsecond aperture the galaxy has the following magnitudes:
$B = 26.13 \pm 0.17$, $V = 25.85 \pm 0.22$, $R_C = 26.31 \pm 0.25$
$I_C = 24.7 \pm 0.4$ (Dodonov et al., 2001).

However, the detection of the object in the B

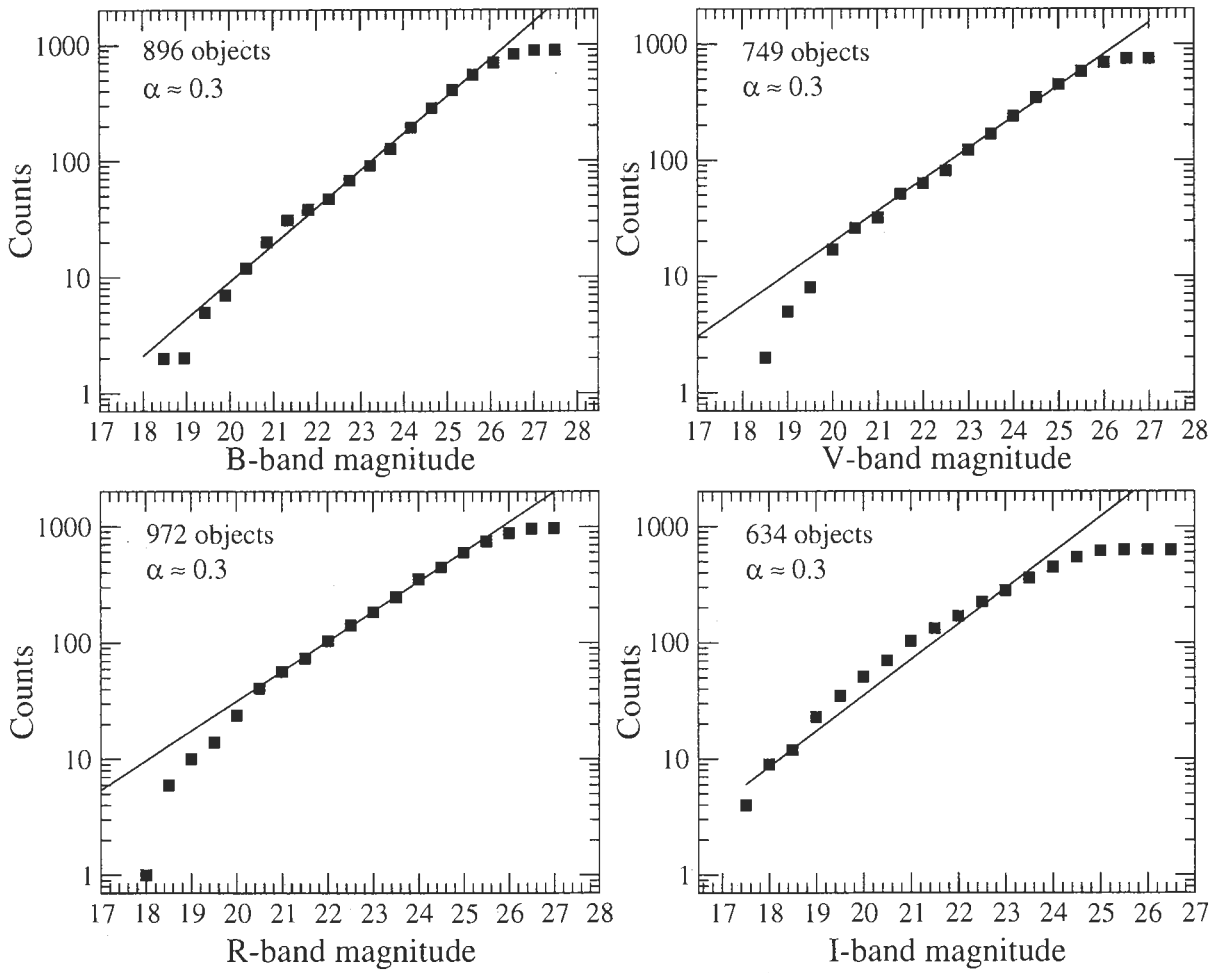

Figure 5: *Integral "magnitude-counts" distributions for objects detected in all bands with $S/N > 4$.*

band by the SExtractor still provides an opportunity to compare its SExtractor magnitude to that reported in Dodonov et al. (2001). Within the two-arcsecond aperture the SExtractor measured magnitude is 25.80 ± 0.14. However, as we have the B-band magnitude only, we should take into account the uncertainty caused by the color term absence in the instrumental-to-standard transformation. Following the RMS of the color distribution its value is not greater than 0.1 magnitude. Thus, the magnitude measured by SExtractor is 25.80 ± 0.18, which within 1σ is in agreement with the magnitude obtained by hand. Note that the small difference in the magnitudes is, in principle, possible, because of the methods of determination of the aperture center (Gauss approximation of intensity distribution of the object profile or the mean weighted with intensity distribution).

Observations of the GRB 000926 optical transient and the host galaxy were also performed with the Hubble Space Telescope and WFPC2 (Price et al., 2001; Harrison et al., 2001; Castro et al., 2001). The final HST epoch data were obtained on UT May 19.63–19.86, 2001 (about two month prior to our observations) in the F450W, F606W and F814W bands (Castro et al., 2001). Transformation of the HST SMAG magnitudes measured within the aperture radius $0''.25$ to the standard Johnson-Cousins ones gives the following results (see Table 4 in Castro et al., 2001): $B = 25.86 \pm 0.14$, $V = 25.66 \pm 0.05$, $R_C = 25.29 \pm 0.06$ and $I_C = 24.95 \pm 0.06$. Note that the quoted errors are statistical only (Castro et al., 2001). In the B, V and I_C bands these magnitudes are in good agreement within the uncertainties with our photometry. The consistency of the magnitudes allows us to consider that we observed, indeed, a constant source, i.e. the host galaxy. It should be noted that our R_C magnitude is about 1^m fainter than the HST one. This magnitude inconsistency might be caused by several reasons. Firstly, one may suppose that this is due to some feature on the SCORPIO CCD (e.g. bad pixel). But this explanation can be rejected because the telescope was shifted by about 9 arcsec (30 CCD pixels) between each exposure in the course of observations (see Sect. 2). Another reason may follow from possible uncertainties of the method

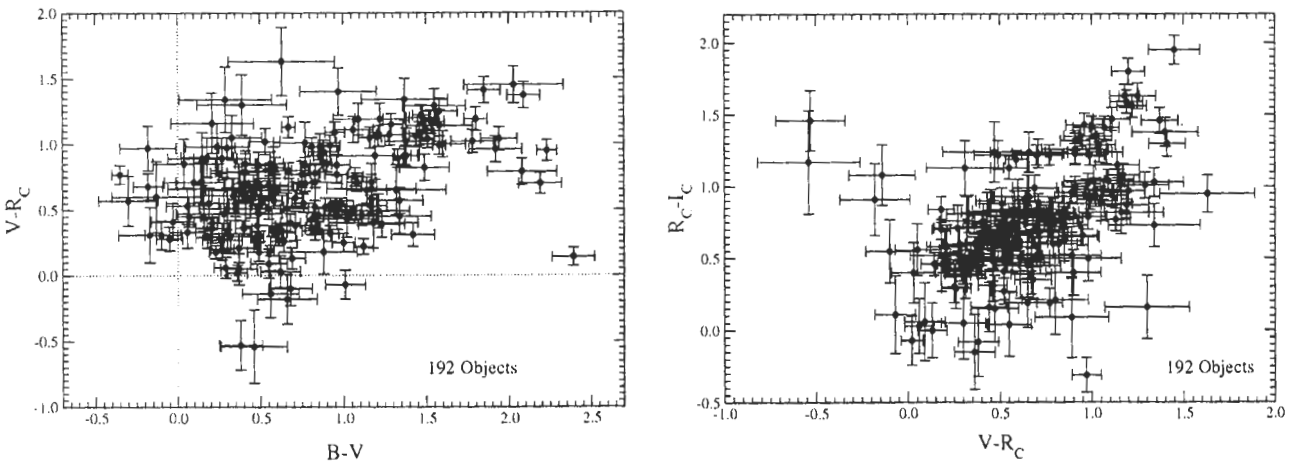

Figure 6: *The two-color diagrams for all the objects with a $S/N > 4$ in the common field. (As a demonstration of color errors, because colors are most useful for a wide range of tasks).*

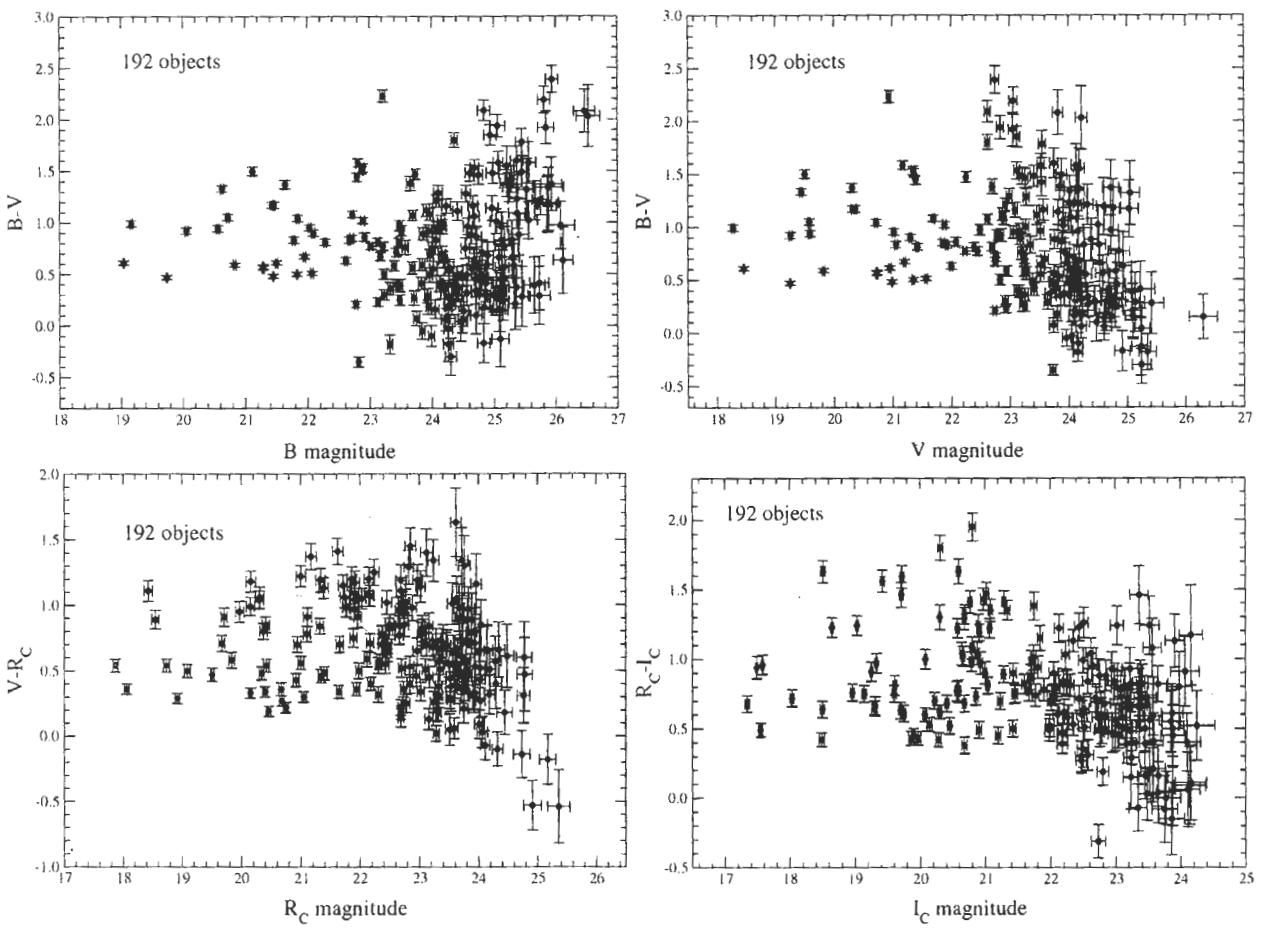

Figure 7: *The "magnitude–color" diagrams for all the objects with a $S/N > 4$ in the common field.*

used by Castro et al. (2001) for transformation from HST F606W and F814W to Johnson-Cousins R_C based on Holtzman et al. (1995) definition. In accordance with Table 10 from Holtzman et al. (1995) one is not allowed to obtain the R_C-band magnitude directly from the F606W and F814W bands. Probably, the HST R_C magnitude was obtained by interpolating between the V and I_C bands and assuming a

smooth host galaxy spectral energy distribution, but the authors did not discuss this. Alternatively, it can be supposed that there is some absorption feature in the host galaxy continuous spectrum. It is interesting that for the host galaxy redshift $z = 2.0379$ (Castro et al., 2001), the graphite absorption "bump" at 2200Å in a "Milky Way"-like extinction curve falls exactly in the observed R_C band. As was shown by modeling of spectral energy distribution of the GRB 980703 host galaxy (Sokolov et al., 2001), this feature can actually be present. But we stress that the deficit of the R_C-band flux must be checked by data with a higher S/N ratio.

It is interesting to compare the colors of the host galaxy to the colors of the field objects. For this purpose, we chose the objects with magnitudes $B > 25^m$ from the "$S/N > 4$" catalog. All the chosen objects are extended in accordance with the `STAR CLASS` parameter. This comparison of $B-V$ and $V-I_C$ colors is shown in Fig. 13. Our choice of the $B-V$ and $V-I_C$ colors is explained by an uncertainty in the R_C-band magnitude as was discussed above.

As one can see from Fig. 13, the colors of the host galaxy occupy the "blue part" of the field galaxy color distribution. Naturally this effect can be explained by star formation in the host galaxy, which, in turn, supports the scenario of a massive star to be a progenitor of gamma-ray bursts.

5. Conclusion

It should be stressed in conclusion, that the main goal of the paper was demonstration of possibilities of field photometry in GRB host galaxy fields. The results showed that deep photometric limits were achieved indeed. The method of object classification by colors was demonstrated. Moreover, we made a comparison of the host galaxy colors with the field objects' colors. We showed by this that the host galaxy does not exhibit any color peculiarity, at least for the $B-V$ and $V-I_C$ colors (see Fig. 13), but for the unusual behavior of the host galaxy continuum in the R_C band. Nevertheless, it seems that the GRB 000926 host galaxy is a typical object for its epoch (redshift).

Acknowledgements. The author thanks V.N. Komarova, S.N. Dodonov, V.L. Afanasiev and A.V. Moiseev for obtaining observational data and help in photometry. This work was done within the frame of the Ph.D. theme "Photometric study of GRB host galaxies" of T.A. Fatkhullin.

References

Adelberger K.L., Steidel C.C., 2000, Astrophys. J., **544**, 218

Berger E., 2001, to appear in proceedings of the "Gamma-Ray Burst and Afterglow Astronomy 2001: A Workshop Celebrating the First Year of the HETE Mission", Woods Hole; 5–9 Nov., 2001, `astro-ph/0112559`, `http://xxx.lanl.gov`

Bertin E., Arnouts S., 1996, Astron. Astrophys. Suppl. Ser., **117**, 393

Bessel M.S., 1990, Publ. Astr. Soc. Pacific, **102**, 1181

Blain A.W., Natarajan P., 2000, Mon. Not. R. Astron. Soc., **312**, L35–L38

Castro S., Galama T.J., Harrison F.A., et al., 2001, submitted to the Astrophys. J., `astro-ph/0110566`, `http://xxx.lanl.gov`

Dodonov S.N., Fatkhullin T.A., Sokolov V.V., et al., 2001, GCN No. 1091, `http://gcn.gsfc.nasa.gov`

Fukugita M., Shimasaku K., Ichikawa T., 1995, Publ. Astr. Soc. Pacific, **107**, 945

Harrison F.A., Yost S.A., Sari R., et al., 2001, Astrophys. J., **559**, 123

Holtzman I.A., Burrows C.J., Casertano S., et al., 1995, Publ. Astr. Soc. Pacific, **107**, 1065

Kron R.G., 1980, Astrophys. J. Suppl. Ser., **43**, 305

Landolt A.U., 1992, Astron. J., **104**, 340

Neizvestny S.I., 1983, Astrofiz. Issled. (Izv. SAO), **17**, 26

Price P.A., Harrison F.A., Galama T.J., et al., 2001, Astrophys. J., **549**, L7–L10

Ramirez-Ruiz E., Fenimore E.E., Trentham N., 2000, talk given at the CAPP2000 Conference on Cosmology and Particle Physics, Verbier, Switzerland, `astro-ph/0010588`, `http://xxx.lanl.gov`

Sokolov V.V., Fatkhullin T.A., Castro-Tirado A.J. et al., 2001, Astron. Astrophys., **372**, 438

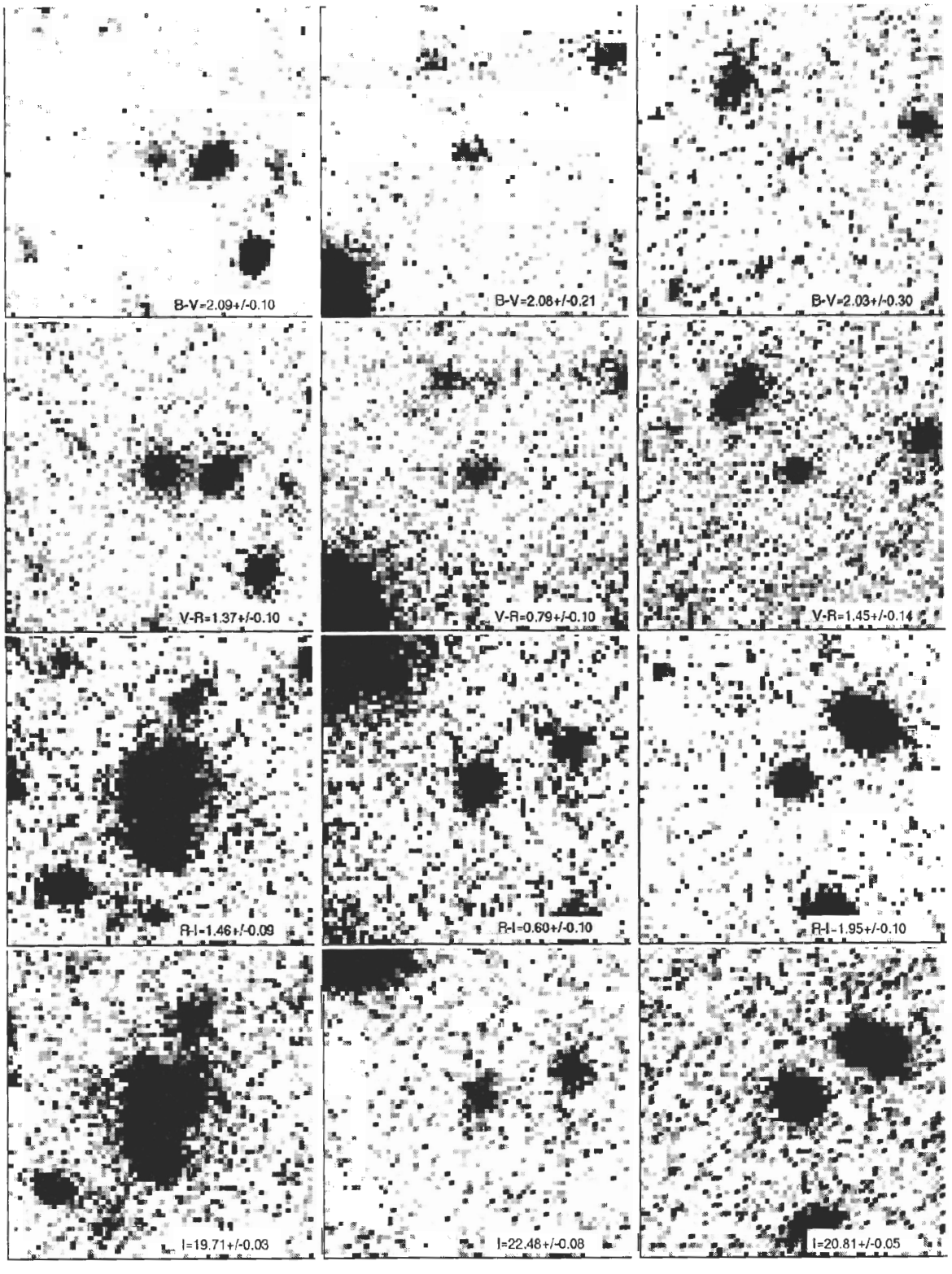

Figure 8: *Examples of the reddest objects ($B-V>2.0$, the first row is the B-band, the second is the V-band, the third is the R_C-band and the lower is the I_C-band).*

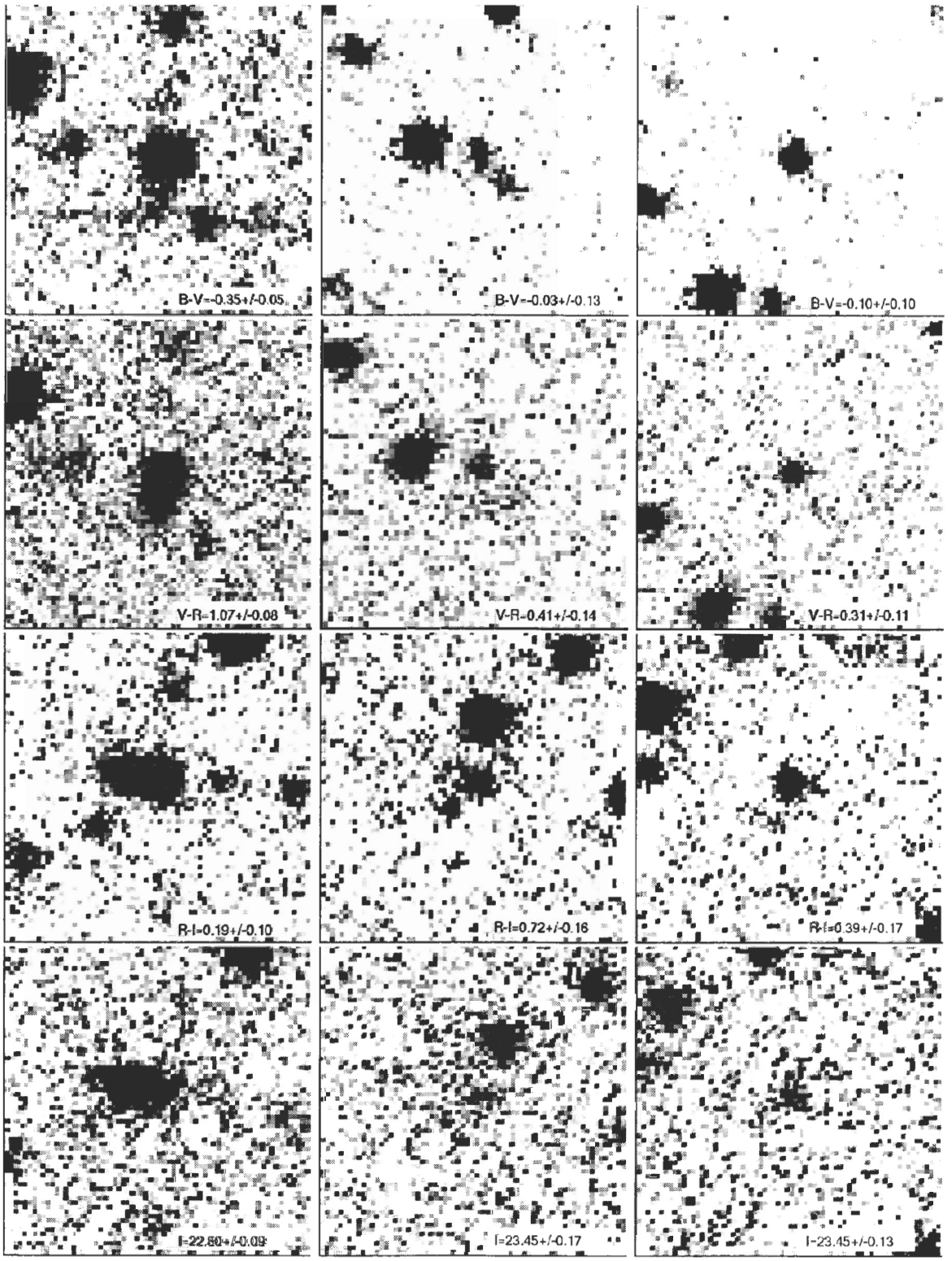

Figure 9: *Examples of the bluest objects ($B - V < 0.0$, the first row is the B-band, the second is the V-band, the third is the R_C-band and the lower is the I_C-band).*

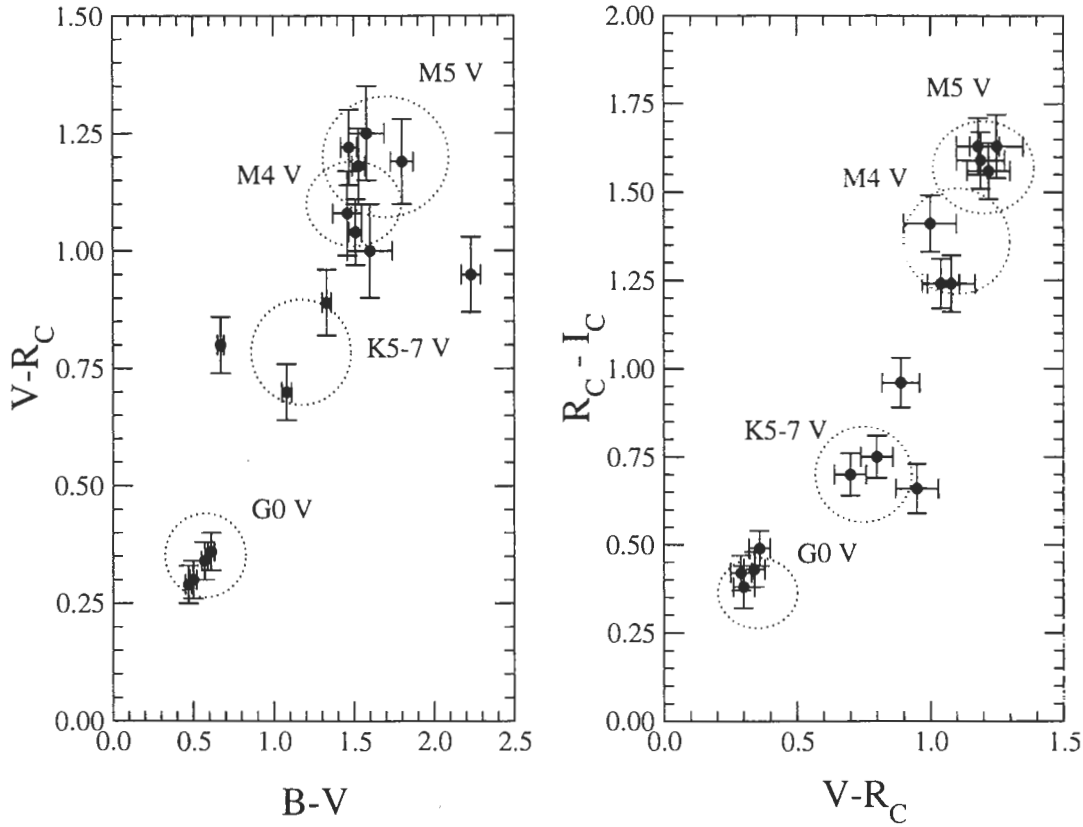

Figure 10: *Colors of the star-like objects in the common field. Classification is also shown. As can be seen, the colors of almost all the objects are good represented by colors of the main-sequence dwarfs.*

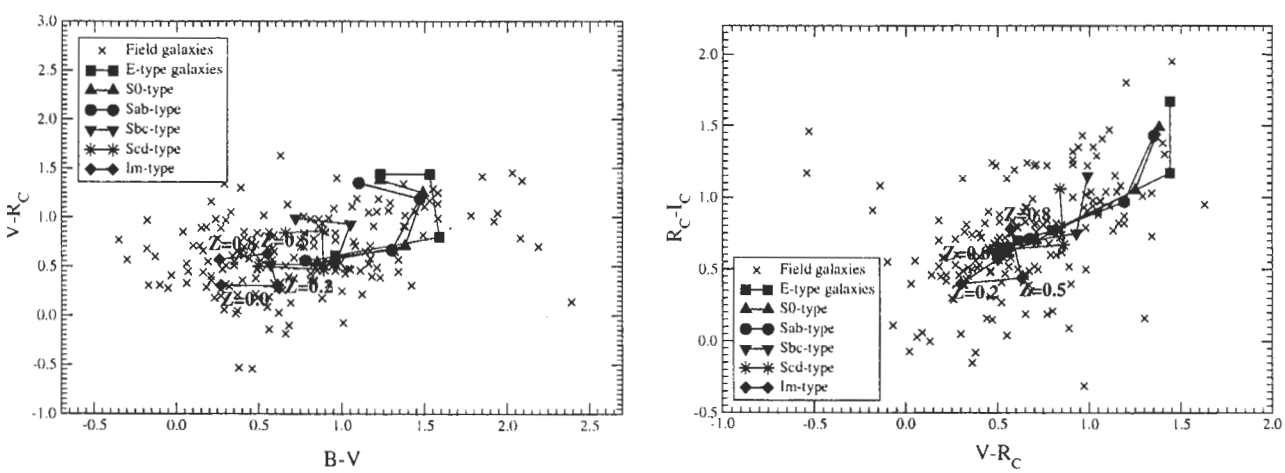

Figure 11: *Comparison of the extended object colors in the common field with the colors of galaxies of different Hubble types on different redshifts ($z = 0.0, 0.2, 0.5, 0.8$). The colors of the majority of the extended objects correspond to those of galaxies with a redshift up to ~ 1.*

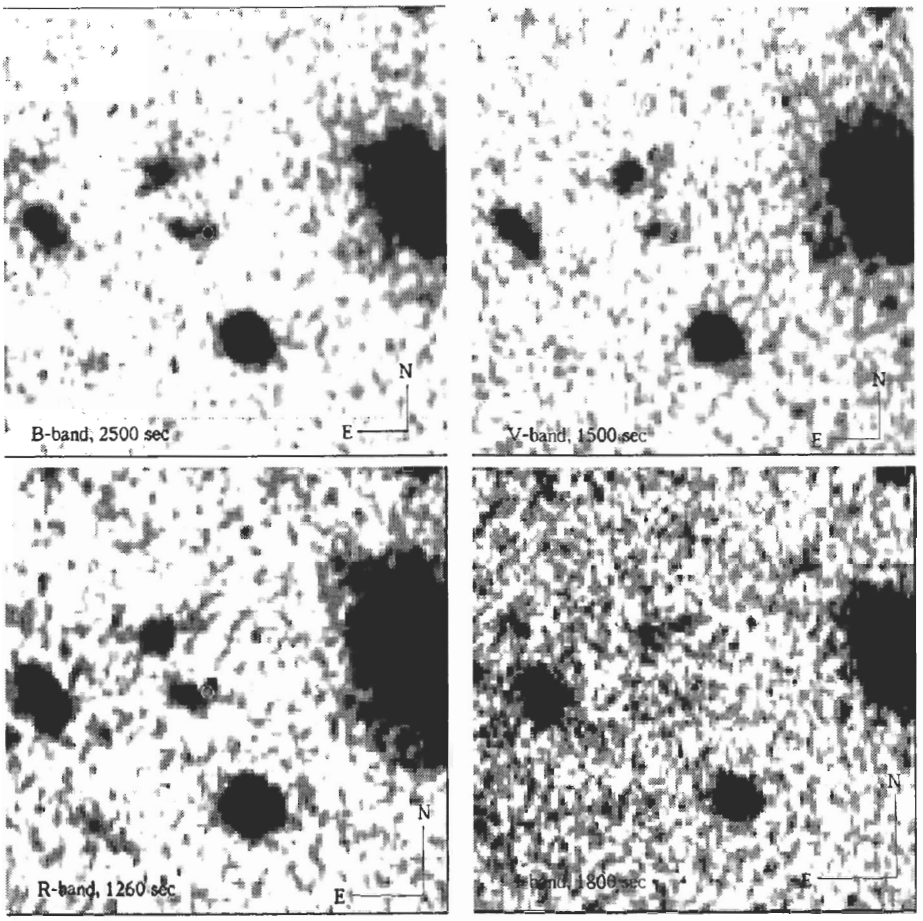

Figure 12: *The* 30×30 *arcsec neighbourhood of the GRB 000926 host galaxy. The circle marks the position of the optical transient (size is 1 arcsec in accordance to astrometrical error).*

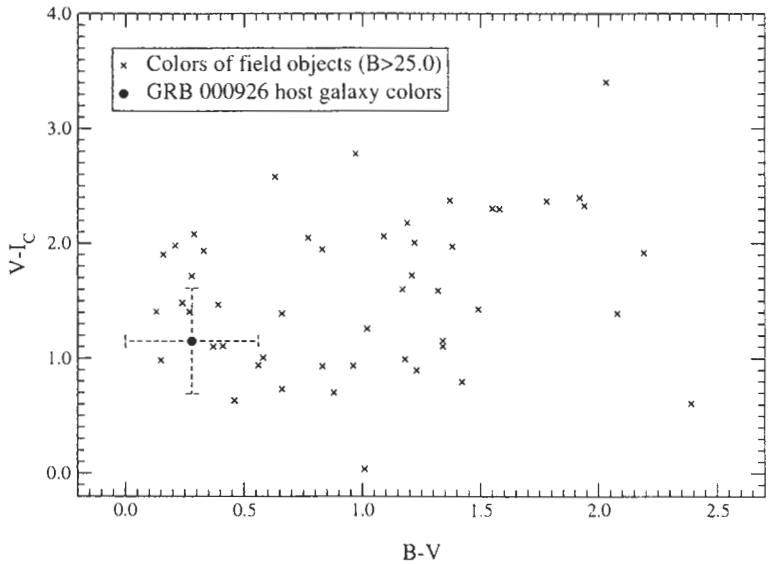

Figure 13: *Comparison of the GRB 000926 host galaxy colors with the colors of the field objects with the same magnitudes* ($B > 25^m$).

БИБЛИОТЕКА